Dental Materials Journal 25(1) : 13−19, 2006

Abrading Increases Oxygen and Hardness of Titanium Surface

Osamu MIYAKAWA[1], Seigo OKAWA[1] and Masayoshi KOBAYASHI[2]
[1]Division of Biomaterial Science, Course for Oral Life Science, Niigata University Graduate School of Medical and Dental Sciences, Gakkou-cho-dori 2-5274, Niigata 951-8514, Japan
[2]EPMA Laboratory, Niigata University Center for Instrumental Analysis, Gakkou-cho-dori 2-5274, Niigata 951-8514, Japan
Corresponding author, Osamu Miyakawa E-mail:miya@dent.niigata-u.ac.jp

Received September 29, 2005/Accepted November 7, 2005

CP Ti was mirror-polished and then abraded with waterproof SiC papers of two different grit sizes: 16 and 3 μm. As-polished and abraded surfaces were characterized by means of EPMA, XPS, XRD, and hardness test.

Oxygen in the mirror-polished surface was uniformly distributed at the lowest level. Comparatively, abrading with SiC papers increased the surface oxygen amount and hardness.

Owing to its excellent abrasivity, the coarse grit efficiently scratched the surface and hindered the regenerated oxide film from growing thick, but allowed only the metal-oxide interfacial gradient zone to extend. But, the fine grit merely rubbed the surface and allowed both the oxide film and interfacial zone to extend. Further, the surface appeared to be lightly yellow-colored, suggesting that the oxide film was thicker, probably within 10 nm, than the nominal one.

When compared with the bulk, the interfacial zone was rich in oxygen and therefore subjected to high coherency strain, which was introduced to relieve the great lattice mismatch between the outer and inner layers of titanium substrate. Effects of solute oxygen hardening and strain hardening were speculated to be responsible for the surface hardening of both SiC-abraded surfaces. In conclusion, abrading with a coarse grit led to accumulation of a high, non-uniform strain in the titanium substrate, thereby hardening the surface further.

Key words: Titanium, Abrading, Oxygen

INTRODUCTION

Well known for its corrosion resistance, titanium poises itself as a promising biomaterial. Its application has since been extended to dental implants and jaw reconstruction because of its excellent biocompatibility. With a view to widening its range of applications, attention has been paid to address its various problems. Some of the problems to be tackled include improvement of corrosion resistance[1,2], development of new investment materials for titanium casting[3−6], clarification of molten titanium flow in casting mold[7−9], application of laser welding technique to extended prostheses[10,11], and surface modification for high resin-titanium bonding strength[12,13].

However, since titanium has low thermal conductivity, heat that is generated due to interaction with cutting tool does not dissipate quickly, thus causing the temperature at cutting point to rise high. Under such conditions, the tool is prone to react with inherently reactive titanium and thereby undergo severe chemical wear. Against this background, the machinability and grindability of titanium and its alloys pose a special challenge[14−16]. These processing difficulties have greatly limited its clinical applications in dentistry[17]. To circumvent this limitation, some machinable titanium alloys have been developed in the dental field[18−21].

Similarly, titanium is not easy to mirror-finish, as it has been so reported in previous studies[22−26]. Finishing with papers of fine SiC grit[22] or a lapping film of α-Al_2O_3 grit (9 μm)[24] caused silicon or aluminum to be incorporated into the surface, which was always accompanied with an increase in surface oxygen amount. Likewise, when the surface was polished using superfine Fe_2O_3 slurry under relatively high pressure, similar effects were reported[25]. Electrochemical buffing with α-Al_2O_3 slurry[26] created a smooth and chemically clean (at EPMA level) surface, whereas mechanical buffing alone yielded a relatively rough surface containing substantial amounts of aluminum and oxygen. Such changes of surface composition may influence titanium's *in vivo* corrosion resistance and biocompatibility.

The present study focused on the increases in oxygen amount and hardness of titanium surface abraded with waterproof papers of coarse and fine SiC grits. The abraded surfaces were characterized by means of electron probe microanalysis (EPMA), X-ray photoelectron spectroscopy (XPS), X-ray diffraction (XRD), and Vickers microhardness test. Results were discussed in relation to extensions of oxide film and oxide-metal interfacial gradient zone. Strain hardening due to abrading-induced micro plastic deformation was also taken into consideration.

MATERIALS AND METHODS

Preparation of specimens

Specimens were as-received ingots of CP Ti (Pure Ti-

tanium A, Morita, Kyoto, Japan), equivalent to Class 2 classified in JIS (Japanese Industrial Standard). Specimen size was 20 mm in diameter and 5 mm in height. In a polishing machine (AUTOMAX, Refine Tec, Yokohama, Japan), the specimens were progressively abraded with waterproof SiC papers up to #600 grit under running tap water, and then mirror-polished with superfine Fe_2O_3 slurry under light pressure.

Subsequently, specimens were abraded under finger pressure on waterproof SiC papers of two different grit sizes: #1000 (LCCD-PS 1000, Sankyo Rikagaku, Tokyo, Japan) and UF 1200 (FEPA: 4000) (30-5528-012, Buehler, IL, USA). The mesh number notation employed in JIS is different from that in USA CAMI[27]. According to these specifications, the respective grit sizes were 16 and 3 μm respectively — and the size difference was unexpectedly wide (Fig. 1). Hereafter, they will be denoted as SIC/16 and SIC/03. Using load cell calibration, finger (abrading) pressure was found to range from approximately 3.0 to 3.5 g/mm^2. Rotational speed of abrasive paper was 130 rpm, and the abrading time was three minutes. Finally, all specimens were ultrasonically rinsed in acetone for 300 seconds. Mirror-polished surfaces served as control.

Element analysis by EPMA

Element analyses for titanium, silicon, and oxygen were performed in stage scan mode under the following conditions: accelerating voltage=20 kV, specimen current=0.2 μA, scanning step interval=1 μm, and sampling time=0.05 s/step (EPMA-8705 H-II, Shimadzu, Kyoto, Japan). For titanium, K_β line was acquired instead of K_α line as the latter's intensity was too high to be counted precisely due to loss of count by the detector. To evaluate the amount of surface oxygen, an artificially prepared spectroscopic crystal (LSA, Shimadzu, Kyoto, Japan) was used, which was 10 times or more as sensitive as rubidium acid phthalate (RAP) crystal.

Surface texture of the element-analyzed areas was also observed through back-scattered electron (BSE) or secondary electron (SE) images.

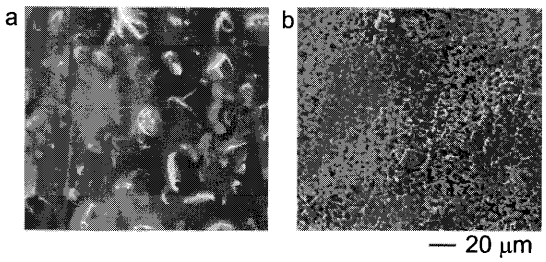

Fig. 1 SE images of SiC papers: (a) #1000 grit and (b) UF 1200 grit.

EPMA state analysis of oxygen

O K_α spectra from SiC-abraded surfaces were acquired by RAP crystal with a low noise level. The obtained profiles were compared with two references: rutile and α-case of titanium casting. The former is one of the titanium oxides, and the latter is rich in solute oxygen. This state analysis was conducted at three points (diameter: 20 μm) randomly chosen on each specimen, thereby confirming the reproducibility.

XPS state analysis

Mirror-finished surfaces were cleaned by Ar^+ ion sputtering for 100 seconds, and then abraded with SIC/16 or SIC/03 paper. Subsequently to this, depth profiling of O 1s was performed (JPS-71XPS1, JEOL, Tokyo, Japan). Sputtering rate calibrated with silica as reference was 0.588 nm/s. X-ray source for excitation was Mg K_α generated under a power of 10 kV and 20 mA. Analyzed area was 6 mm in diameter and partly pre-sputtered with gold for calibration of peak shift due to surface electron charging. The analyzing chamber was kept at a vacuum of 1 μPa, but Ar gas of 3×10^{-2} Pa was introduced into the sputtering chamber.

SIC/16 surface was analyzed for depth profiles of Si 2p and Ti 2p. In this analysis, sputtering rate calibrated with silica as reference was 0.21 nm/s.

Determination of lattice parameters of titanium by XRD

Lattice parameters of titanium substrate were determined by XRD (Geigerflex, Rigaku, Tokyo, Japan). X-ray source was Ni-filtered Cu K_α generated at a power of 40 kV and 30 mA. Diffracted X-rays were acquired over a 2θ range of 50 to 80° under the following conditions: divergent slit=1°, receiving slit=0.15 mm, scattering slit=1°, rotating speed of goniometer=0.5°/min, time constant=2 s, and chart speed=10 mm/min.

Hardness test

One specimen was prepared for each condition. Vickers microhardness was tested at 10 points randomly chosen on each specimen (MVK Type C, Akashi, Zama, Japan). Indentation load was 100 g and the retention time was 30 seconds. Results were analyzed by one-way ANOVA, followed by post-hoc Tukey's test.

RESULTS

Surface texture

Control surface was metallic glossy, although slight undulation was observed (Fig. 2a). SIC/16 surface was rough and unglossy due to a number of scratch lines (Fig. 2b). SIC/03 surface was rather smooth, although several dulled scratch lines remained (Fig.

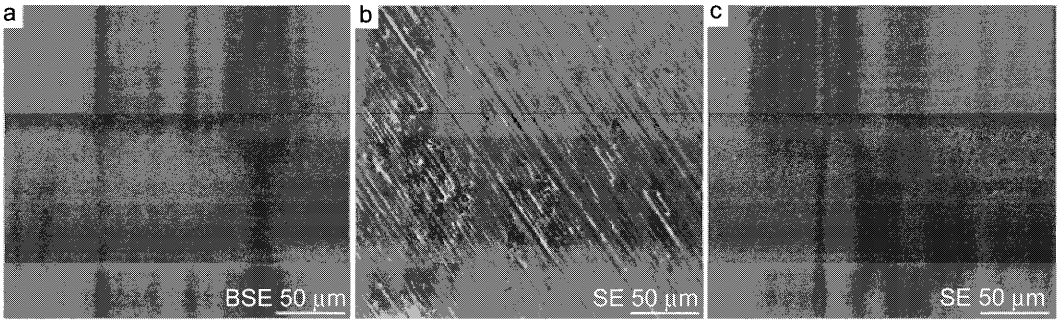

Fig. 2 BSE or SE images of: (a) mirror-polished; (b) SIC/16; and (c) SIC/03 surfaces.

2c). Interestingly, the surface was metallic glossy and lightly yellow-colored.

Surface composition

Ti K_β and O K_α from the control surface showed uniform intensity distributions of the highest and lowest levels (2,050 and 50 counts), respectively (Fig. 3a).

Ti K_β intensity from SIC/16 surface decreased and varied between 1,600 and 1,800 counts (Fig. 3b). Si K_α and increased O K_α intensities varied widely with reverse correspondences to Ti K_β. However, no exact correlations were found between variations of these three elements, which might partly result from the rough surface texture, as the directions normal to abraded slopes were different from point to point with respect to the location of each element detector.

Ti K_β from SIC/03 surface showed an almost uniform intensity distribution, of which the level was lower by approximately 10% than that from the control surface (Fig. 3c). Si K_α level was low and in accordance with its background, except for one point where an abrasive grit was probably stuck in the surface. It should be noted that O K_α intensity was extremely high as a whole and showed a variation between approximately 140 and 200 counts.

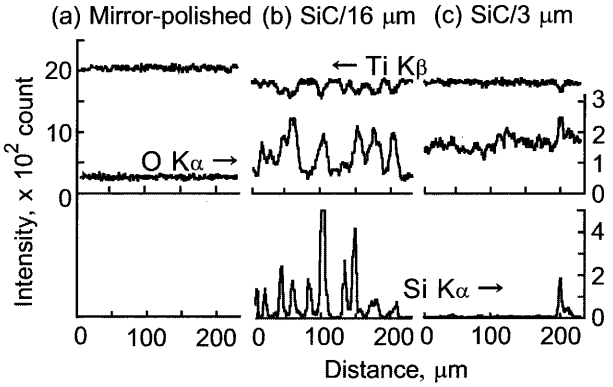

Fig. 3 Line profiles showing variations of Ti K_β, O K_α, and Si K_α intensities from: (a) mirror-polished; (b) SIC/16; and (c) SIC/03 surfaces. These profiles were depicted along horizontal lines at 1/2, 1/5, and 2/5 height of the corresponding images shown in Fig. 2.

EPMA state analysis of oxygen

O K_α spectrum from SIC/16 surface had a peak at the longer wavelength side, hence similar to that from α-case of titanium casting (Fig. 4). The spectrum from SIC/03 surface had an additional component at the shorter wavelength side, hence rather similar to that from rutile.

XPS state analysis

The outermost surface of as-sputtered specimen was somewhat rich in OH^- or H_2O, whereas that of SiC-abraded specimens was rich in O^{2-} (Fig. 5). However, O^{2-} was a major component in the deeper region of all specimens.

Irrespective of surface treatment, O 1s peak remained after the final sputtering, as the pressure in the sputtering chamber was too high to prevent oxygen from adsorbing on titanium surface. Nonetheless, around sputtering times shown by arrows, each

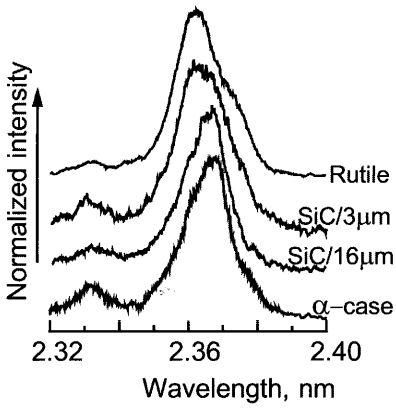

Fig. 4 O K_α spectra from SIC/16 and SIC/03 surfaces.

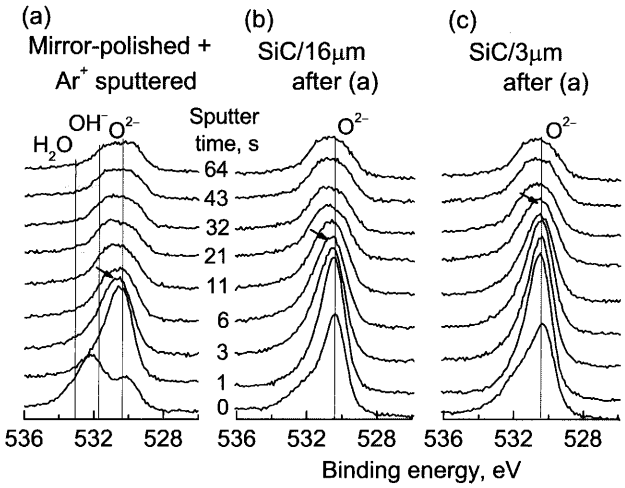

Fig. 5 Depth profiles of O 1s from: (a) sputter-cleaned; (b) SIC/16; and (c) SIC/03 surfaces. Arrows show depths at which O 1s peak started shifting from the peak position of O^{2-} to the higher energy side.

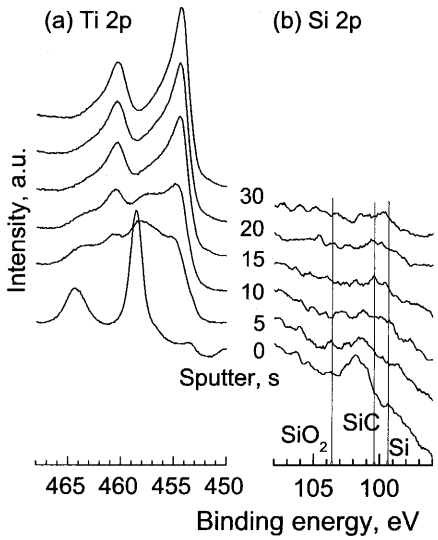

Fig. 6 Depth profiles of: (a) Ti 2p and (b) Si 2p from SIC/16 surface.

O 1s peak started shifting from the peak position of O^{2-} ion to the higher energy side. Accordingly, thickness of the oxide film was concluded to be in the order of control < SIC/16 < SIC/03 surface.

Silicon was chiefly present in the outermost layer of SIC/16 surface (Fig. 6). The silicon contaminant was entirely different from SiC in chemical bonding. A small amount of silicon might be caused by a knock-on phenomenon.

Lattice parameters of titanium substrate

All XRD peaks were assigned to α-titanium (Fig. 7). Each peak individually had a right-sided shoulder showing incomplete $K_{\alpha 1}$-$K_{\alpha 2}$ split. As compared with the control surface, the corresponding peaks from both SiC-abraded surfaces were shifted to the lower angle side, hence suggesting the extension of titanium lattice. As indicated by vertical lines, the positions of $K_{\alpha 1}$-induced peaks were registered, and the lattice parameters for each specimen were determined by the least squares method (Table 1).

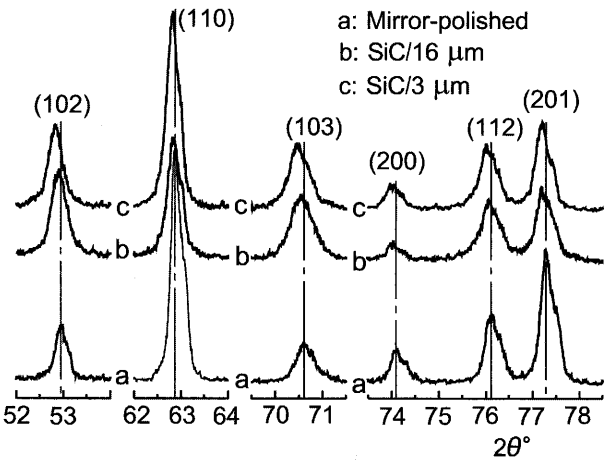

Fig. 7 XRD charts of: (a) mirror-polished; (b) SIC/16; and (c) SIC/03 surfaces. $K_{\alpha 1}$-$K_{\alpha 2}$ split was assumed and $K_{\alpha 1}$-peak positions from mirror-polished surface were estimated (vertical lines).

Table 1 Lattice parameters of titanium (in nm)

	a	c	Δ/N
JCPDS #44-1294	0.2950	0.4682	—
Mirror-polished	0.2954	0.4687	0.000030
SIC/16-abraded	0.2956	0.4693	0.000023
SIC/03-abraded	0.2957	0.4694	0.000020

$\Delta^2 = \Sigma_{hkil}[d_{hkil} - a/\{4(h^2+hk+k^2)/3+(a/c)^2 l^2\}^{1/2}]^2$,
where d_{hkil} were values measured from XRD chart; a and c were determined from (102), (110), (103), (112), and (201) peaks by Least Squares Method.

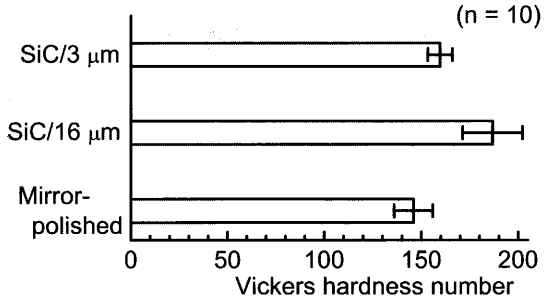

Fig. 8 Vickers microhardness of mirror-polished, SIC/16, and SIC/03 surfaces.

Hardness of abraded surfaces

In comparison with the control surface, abrading with SiC papers hardened the titanium surface ($p<0.05$) (Fig. 8). SIC/16 surface was significantly harder than SIC/03 surface ($p<0.05$).

DISCUSSION

In previous studies of high-pressure abrading or polishing, oxide abrasives such as Al_2O_3[24], Fe_2O_3[25], and Cr_2O_3[28] have been reported to increase the oxygen amount in titanium surface. In the present study, it was noted that non-oxide abrasive also had a similar effect (Fig. 3).

O K_α spectra from SIC/16 and SIC/03 surfaces were similar to those from α-case of titanium casting and rutile, respectively (Fig. 4). To account for the difference, individual contributions of solute oxygen and oxide-constituent oxygen to O K_α spectrum were assessed as follows:

Oxygen amount per unit area in a layer is represented by

$$\boldsymbol{dBW}/100, \quad (1)$$

where $\boldsymbol{d}$ is thickness of layer, $\boldsymbol{B}$ is density, and $\boldsymbol{W}$ is oxygen concentration expressed as weight percentage. The oxygen amount in 4-nm thick oxide film was calculated as $0.79\,\mu g/cm^2$, assuming that the film comprised TiO_2 ($\boldsymbol{B}=4.93$ g/cm^3 and $\boldsymbol{W}\approx 40$ wt%). On the other hand, the titanium ($\boldsymbol{B}=4.54$ g/cm^3) used in this study is allowed to contain 0.15 wt% oxygen at maximum. The analysis depth of EPMA depends on the penetration depth of applied electron beam, generally a few micrometers. Assuming that the analysis depth of oxygen in titanium was $1.5\,\mu m$, the oxygen amount in the titanium substrate was calculated as $1.0\,\mu g/cm^2$. Thus, when oxide film thickened from 4 to 8 nm, the contribution of the oxide to O K_α spectrum would increase from 44 to 61%. Although O K_α absorption in substances was ignored and some assumptions were introduced, this simplified model was enough to account for the difference in O K_α profile between SIC/16 and SIC/03 surfaces.

In electromechanical buffing, titanium becomes gold-colored when voltage higher than 5 V is applied[26]. However, despite being treated in non-electric field, titanium was lightly yellow-colored when it was abraded with SIC/03 paper. This implied that the oxide film on SIC/03 surface was thicker, probably within 10 nm, than the nominal one[29]. Moreover, XPS results also showed that the oxide film on SIC/03 surface was thicker than that on SIC/16 surface (Fig. 5). Thus, EPMA and XPS results, together with the occurrence or non-occurrence of coloring, were mutually compatible. In summary, SIC/16 paper preferentially increased the solute oxygen amount, whereas SIC/03 paper thickened the oxide film and probably increased the solute oxygen amount.

As compared with the control surface, XRD peaks from both SiC-abraded surfaces, except for (102) and (103) peaks, were to a certain extent low and broad (Fig. 7). This broadness was probably caused by non-uniform strain that was accumulated in titanium substrate through abrading-induced micro plastic deformation. Moreover, all peaks from both SiC-abraded surfaces were shifted to the lower angle side − more noticeably for peaks with higher index l. α-titanium lattice size is known to extend with increasing solute oxygen concentration, in particular in c-direction[30]. According to a reference[30], the determined c value (e.g., 0.4693 nm) (Table 1) seemingly corresponded to approximately 2 at% (0.67 wt%) oxygen, which was much higher than the maximum limit (0.15 wt%) specified in JIS. Based on the absorption coefficient of Cu K_α passing through titanium, the analysis depth of XRD was approximately $5\,\mu m$ at $2\theta = 60°$. However, it was impossible that abrading led to the augmentation of oxygen up to 0.67 wt% over this depth range. Thus, to propose a hypothesis for the mechanism of lattice extension, attention was paid to the oxide-metal interfacial gradient zone.

The thickness of interfacial zone determined by Rutherford backscattering spectroscopy (RBS) is 39 ±2 nm for a polished CP Ti sample[31,32]. It is thicker by one order of magnitude than the layer of TiO_2 stoichiometry itself. Moreover, RBS study of anodic-oxidized surface below breakdown limit has demonstrated that the interfacial zone is able to extend two to three times the nominal thickness into the metal[33]. This suggests oxygen dissolution in titanium with a large diffusion coefficient. Assuming that TiO layer is present between TiO_2 film and titanium substrate, the oxygen concentration must sharply change from approximately 25 to 0.15 wt% over the interfacial zone. This step-like change would bring about a potential situation that the outer layer of titanium substrate had a much larger lattice size than the inner layer, hence causing a very

great lattice mismatch ranging from the interfacial zone to its underlying layer. This mismatch must be relieved, thus resulting in the formation of coherency strain where inherently larger lattices in the outer layer were obliged to contract, while those in the inner layer to extend substantially. This hypothesis of coherency strain reasonably accounted for the observed XRD peak shifts or lattice size extension. Based on XRD results, the interfacial zones of both SiC-abraded specimens seemed to extend to a similar degree.

Both SiC-abraded surfaces were significantly harder than the control surface, especially the SIC/16 surface (Fig. 8). In general, indentation depth of Vickers microhardness test is within the range of several tens to several hundreds of micrometers. Therefore, the hardness value reflects the mechanical properties averaged over the depth range. In this study, the increase in oxide film thickness by just several nanometers seemed to be too small to account for the hardening of SIC/03 surface. In the same manner, it was even more difficult to account for the hardening of SIC/16 surface without any distinct increase in oxide film thickness. Thus, three probable hypotheses were proposed whereby hardening could be due to: (1) increase in solute oxygen, (2) formation of coherency strain, and (3) inducement of non-uniform strain by abrading.

During the abrading process, abrasive particles scratched and removed the surface oxide film. Titanium itself was exposed to the environment, immediately reoxidized, and finally repassivated. In the meantime, O^{2-} ions were transported inward, which potentially served to thicken the oxide film and to extend the interfacial zone into the metal as well. However, SIC/16 grit with excellent abrasivity repeated the removal and subsequent regeneration of oxide film, thereby hindering the oxide film from growing thick and allowing only the interfacial zone to extend (Figs. 4 and 5). On the other hand, SIC/03 grit merely rubbed the surface because of its poor abrasivity, and allowed both the oxide film and interfacial zone to grow thick. Titanium is known to harden with increasing oxygen concentration[34]. Accordingly, the high oxygen concentration in the extended interfacial zone played a partial role in the surface hardening of both SiC-abraded surfaces. Moreover, as discussed in the foregoing paragraph, the extended interfacial zone and its underlying layer were subjected to high coherency strain, which caused a strain hardening effect on both SiC-abraded surfaces.

From visual comparison of surface textures (Fig. 2), it was inevitably assumed that SIC/16 surface was much more severely deformed than SIC/03 surface. The resultant strain hardening effect would cause further hardening of SIC/16 surface (Fig. 8).

Previous studies have shown that change in surface composition was chiefly due to reaction of titanium with abrasive materials[22-26,28]. Similarly, reaction of titanium with SiC yielded some silicon contaminant in the oxide film on SIC/16 surface (Fig. 6). However, the influence of the contaminant on hardness should be negligible because of the thin oxide film thickness.

CONCLUSION

With the mirror-polished surface, oxygen was uniformly distributed at the lowest level. Comparatively, abrading with SiC papers increased the surface oxygen amount and hardness.

Owing to its excellent abrasivity, the coarse grit efficiently scratched the surface and hindered the regenerated oxide film from growing thick, but allowed only the metal-oxide interfacial gradient zone to extend. On the other hand, the fine grit merely rubbed the surface and allowed both the oxide film and interfacial zone to extend. Further, the surface appeared to be lightly yellow-colored although it was abraded in non-electric field, suggesting that the oxide film was thicker, probably within 10 nm, than the nominal one.

When compared with the bulk, the interfacial zone was rich in oxygen and therefore subjected to high coherency strain, which was introduced to relieve the great lattice mismatch between the outer and inner layers of titanium substrate. In terms of surface hardness, effects of solute oxygen hardening and strain hardening were speculated to be responsible for the surface hardening of both SiC-abraded surfaces. In conclusion, abrading with a coarse grit led to accumulation of a high, non-uniform strain in the titanium substrate, thereby hardening the surface further.

REFERENCES

1) Takahashi M, Kikuchi M, Takada Y, Okuno O, Okabe T. Corrosion behavior and microstructures of experimental Ti-Au alloys. Dent Mater J 2004; 23: 109-116.
2) Takemoto S, Hattori M, Yoshinari M, Kawada E, Asami K, Oda Y. Corrosion behavior and surface characterization of Ti-20Cr alloy in a solution containing fluoride. Dent Mater J 2004; 23: 379-386.
3) Nakai A. Study of resin-bonded calcia investment. Part 2: Effect of titanium content on the dimensional change of the investment. Dent Mater J 2002; 21: 191-199.
4) Meng Y, Nakai A, Goto S, Ogura H. Study of resin-bonded calcia investment. Part 3: Hardness of titanium castings. Dent Mater J 2004; 23: 46-52.
5) Takahashi J, Kitahara K, Kubo F. Phosphate-bonded $ZrSiO_4$ investments added with ZrC and ZrN for casting titanium. Dent Mater J 2004; 23: 314-320.
6) Yan M, Takahashi H, Nishimura F. Dimensional accu-

racy and surface property of titanium casting using gypsum-bonded alumina investment. Dent Mater J 2004; 23: 539-544.
7) Sato H, Komatsu M, Miller B, Shimizu H, Fujii H, Okabe T. Mold filling and microhardness of 1% Fe titanium alloys. Dent Mater J 2004; 23: 211-217.
8) Baltag I, Watanabe K, Miyakawa O. Internal porosity of cast titanium removable partial dentures — Influence of sprue direction and diameter on porosity in simplified circumferential clasps. Dent Mater 2005; 21: 530-537.
9) Keanini RG, Watanabe K, Okabe T. Theoretical model of the two-chamber pressure casting process. Metall & Mater Trans B 2005; 36B: 283-292.
10) Fujioka S, Kakimoto K, Inoue T, Okazaki J, Komasa Y. Metallurgical effects on titanium by laser welding on dental stone. Dent Mater J 2003; 22: 581-591.
11) Iwasaki K, Ohkawa S, Rosca ID, Uo M, Tsukasa Akasaka T, Watari F. Distortion of laser welded titanium plates. Dent Mater J 2004; 23: 593-599.
12) Ban S, Kadokawa A, Kanie T, Arikawa H, Fujii K, Tanaka T. Bonding strength and durability of alkaline-treated titanium to veneering resin. Dent Mater J 2004; 23: 424-428.
13) Kibayashi H, Teraoka F, Fujimoto S Nakagawa M, Takahashi J. Surface modification of pure titanium by plasma exposure and its bonding to resin. Dent Mater J 2005; 24: 53-58.
14) Miyakawa O, Watanabe K, Okawa S, Nakano S, Shiokawa N, Kobayashi M, Tamura H. Grinding of titanium. Part 1: Commercial and experimental wheels made of silicon carbide abrasives. J J Dent Mater 1990; 9: 30-41.
15) Miyakawa O, Watanabe K, Okawa S, Nakano S, Shiokawa N, Kobayashi M, Tamura H. Grinding of titanium. Part 2: Commercial vitrified wheels made of alumina abrasives. J J Dent Mater 1990; 9: 42-52.
16) Hotta Y, Miyazaki T, Fujiwara T, Tomita S, Shinya A, Sugai Y, Ogura H. Durability of tungsten carbide burs for the fabrication of titanium crowns using dental CAD/CAM. Dent Mater J 2004; 23: 190-196.
17) ADA council on scientific affairs. Titanium application in dentistry. JADA 2003; 134: 347-349.
18) Kikuchi M, Takahashi M, Okabe T, Okuno O. Grindability of dental cast Ti-Ag and Ti-Cu alloys. Dent Mater J 2003; 22: 191-205.
19) Kikuchi M, Takahashi M, Okuno O. Mechanical properties and grindability of dental cast Ti-Nb alloys. Dent Mater J 2003; 22: 328-342.
20) Kikuchi M, Okuno O. Machinability evaluation of titanium alloys. Dent Mater J 2004; 23: 37-45.
21) Takahashi M, Kikuchi M, Okuno O. Mechanical properties and grindability of experimental Ti-Au alloys. Dent Mater J 2004; 23: 203-210.
22) Miyakawa O, Watanabe K, Okawa S, Kanatani M, Nakano S, Kobayashi M. Surface contamination of titanium by abrading treatment. Dent Mater J 1996; 15: 11-21.
23) Miyakawa O. Reactivity of titanium with abrasive materials and its polishing. J Jpn Prosthodont Soc 1998; 42: 540-546.
24) Miyakawa O, Okawa S, Kobayashi M, Uematsu K. Surface contamination of titanium by abrading treatment. Dentistry in Japan 1998; 34: 90-96.
25) Akhter R, Okawa S, Nakano S, Kobayashi M, Miyakawa O. Surface composition and structure of titanium polished with aqueous slurry of ferric oxide. Dent Mater J 2000; 19: 10-21.
26) Okawa S, Hossain A, Kanatani M, Watanabe K, Miyakawa O. Surface properties of electrochemically buffed titanium casting. Dent Mater J 2004; 23: 504-511.
27) Buehler's '98 catalog. Cutting, grinding, mounting, and polishing supplies for samples preparation: Comparison of grit size of water-proof abrasive papers between USA CAMI and JIS, 1998, p.18.
28) Hossain A, Okawa S, Miyakawa O. Surface composition and texture of titanium polished with colloidal silica suspension and chromic oxide slurry. Dent Mater J 2005; 24: 409-413.
29) Japan titanium society. Processing technology of titanium, Nikkan Kogyo Shinbunsya, Tokyo, 1992, p.191.
30) Murray JL, Wriedt HA. The O-Ti system. In: Monograph series on alloy phase diagrams — Phase diagrams of binary titanium alloys, Murray JL (ed), ASM international, Metals Park, Ohio 44073, 1990, p.211-229.
31) Brunette DM, Tengvall P, Textor M, Thomsen P. Titanium in medicine, Springer, Berlin, 2001, p.154-162.
32) Poilleau J, Devilliers D, Garrido F, Durrand-Vidal S, Mahe E. Structure and composition of passive titanium oxide films. Mater Sci Eng 1997; 47: 235-243.
33) Serroys Y, Sakout T, Gorse D. Anodic oxidation of titanium in 1M H_2SO_4, studied by Rutherford backscattering. Sur Sci 1993; 282: 279-287.
34) Collings EW. The physical metallurgy of titanium alloys, American society for metals, Ohio, 1984, p.141.